

# A comparison between humans and AI at recognizing objects in unusual poses

Netta Ollikka<sup>\* 1</sup> Amro Abbas<sup>2</sup> Andrea Perin<sup>1</sup> Markku Kilpeläinen<sup>† 3</sup> Stéphane Deny<sup>† 1</sup>

## Abstract

Deep learning is closing the gap with human vision on several object recognition benchmarks. Here we investigate this gap for challenging images where objects are seen in unusual poses. We find that humans excel at recognizing objects in such poses. In contrast, state-of-the-art deep networks for vision (EfficientNet, SWAG, ViT, SWIN, BEiT, ConvNext) and state-of-the-art large vision-language models (Claude 3.5, Gemini 1.5, GPT-4) are systematically brittle on unusual poses, with the exception of Gemini showing excellent robustness in that condition. As we limit image exposure time, human performance degrades to the level of deep networks, suggesting that additional mental processes (requiring additional time) are necessary to identify objects in unusual poses. An analysis of error patterns of humans vs. networks reveals that even time-limited humans are dissimilar to feed-forward deep networks. In conclusion, our comparison reveals that humans and deep networks rely on different mechanisms for recognizing objects in unusual poses. Understanding the nature of the mental processes taking place during extra viewing time may be key to reproduce the robustness of human vision *in silico*.

## 1. Introduction

In an era marked by the rapid advancement of deep learning for computer vision, a natural question arises: Can machines meet or even exceed the capabilities of the human visual system? Numerous recent studies have shown that deep networks outperform humans on well-known object recognition benchmarks (e.g., ImageNet: He et al. (2015); Vasudevan et al. (2022); Dehghani et al. (2023)). Deep

networks are even said to outperform humans on *out-of-distribution* recognition tasks (Geirhos et al., 2021), where the images used for evaluation are subjected to distortions that the networks were not specifically trained on.

However, studies that investigate out-of-distribution generalization mostly focus on local distortions (e.g., texture modifications, blur, color modifications) as opposed to transformations that affect the global structure of the image, such as a change in viewpoint. A few studies have investigated the generalization capability of deep networks to recognize objects in various poses, both in non-adversarial (Alcorn et al., 2019; Ibrahim et al., 2022; Abbas & Deny, 2023; Madan et al., 2022) and adversarial settings (Zeng et al., 2019; Madan et al., 2021), and they show a substantial degradation of network performance for unusual poses. However, a direct comparison with human vision has been missing from these studies, leaving open the question of whether humans outperform networks on this task.

Here, we compare human subjects with state-of-the-art deep networks for vision and state-of-the-art large vision-language models at recognizing objects in various poses. We show that—while both humans and networks excel on upright poses—humans substantially outperform networks on unusual poses (except for Google’s Gemini showing exceptional robustness in that condition). As we limit viewing time, humans exhibit a similar brittleness to deep networks on unusual poses, demonstrating the necessity of additional mental processes for analysing these challenging images. Although networks and time-limited humans are both brittle, an analysis of their patterns of error reveals that time-limited humans make different mistakes than networks. In conclusion, our results show that (1) humans are still much more robust than most networks at recognizing objects in unusual poses, (2) time is of the essence for such ability to emerge, and (3) even time-limited humans are dissimilar to deep neural networks.

## 2. Methods

### 2.1. Dataset collection

We collected a dataset of objects viewed in different poses (upright and rotated out-of-plane), to test the ability of humans to recognize these objects, and compare this ability to

corresponding authors: <sup>\*</sup>netta.ollikka@gmail.com, <sup>†</sup>markku.kilpelainen@helsinki.fi, stephane.deny.pro@gmail.com  
<sup>1</sup>Aalto University, Espoo, Finland <sup>2</sup>The African Institute for Mathematical Sciences, Mboure-Thies, Senegal <sup>3</sup>Department of Psychology and Logopedics, University of Helsinki, Finland.

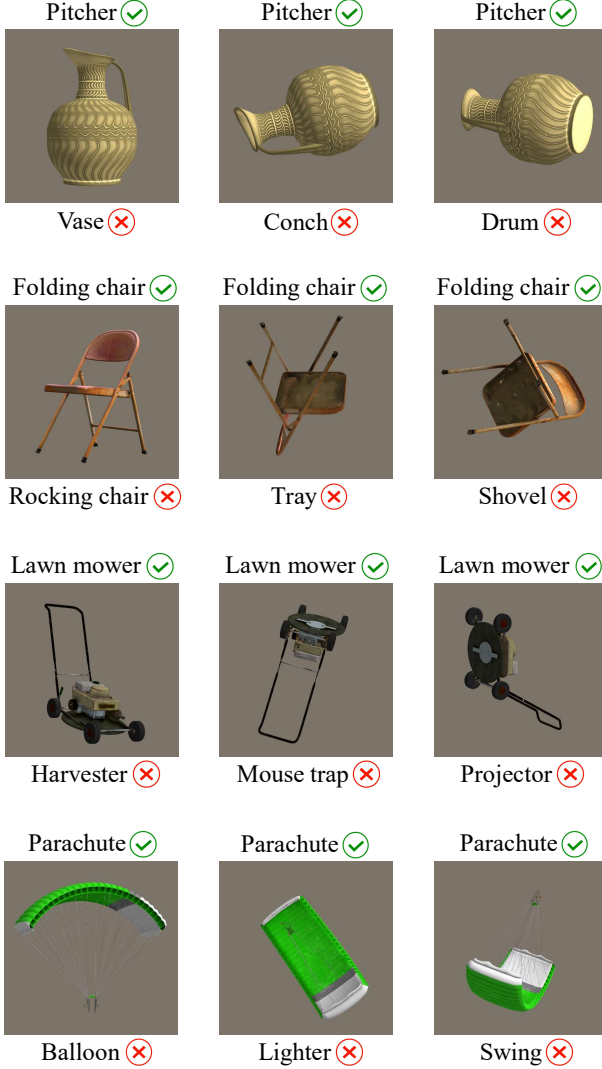


**Figure 1. Example images of the dataset, and corresponding answer choices.** Four examples of objects and their three different rotations: (*left*) upright, (*middle*) rotated and correctly labeled by EfficientNet, and (*right*) rotated and incorrectly labeled by EfficientNet. Above each image is shown the correct label and below each image is the alternative label that we selected based on EfficientNet’s predictions (see *Dataset collection 2.1* for details of this selection).

state-of-the-art deep networks (Figure 1).

We chose 51 different object categories from the ImageNet classes (see *Appendix C* for the list of objects), and obtained a corresponding 3D model for each category from Sketchfab (<https://sketchfab.com/>). The objects were chosen based on a few criteria:

- Objects should look distinct in different rotation angles, e.g., a symmetrical ball wouldn’t be an acceptable

object.

- Objects should have clear upright poses, e.g., a pen wouldn’t be an acceptable object.
- The object in its upright pose should be correctly labeled by Noisy Student EfficientNet-L2, pretrained on JFT-300M and finetuned on ImageNet (Xie et al., 2020) (referred to as EfficientNet below). We chose EfficientNet to guide our selection of objects because it is the best open-source network at recognizing objects in unusual poses, according to a recent comprehensive study comparing 37 state-of-the-art networks on this task (Abbas & Deny, 2023).

Once the objects that satisfy the criteria were chosen, we rendered 180 different random rotations of each one of them (along axis x, y and z). These rotations were given to EfficientNet to be labeled. Then, we performed a selection of poses. First, we selected unusual poses that EfficientNet was able to correctly identify. Second, we selected unusual poses that EfficientNet failed to correctly identify. The dataset thus consisted of three different types of poses: (1) upright, (2) rotated and correctly identified by EfficientNet (rotated-correct condition), and (3) rotated and incorrectly identified by EfficientNet (rotated-incorrect condition).

Once the different poses for each object were chosen, we created two-forced choice questions for each image based on EfficientNet’s predictions. The choices consisted of the correct label, and an incorrect label. In the cases where EfficientNet was able to correctly identify the object, we chose the second best guess of EfficientNet to be the incorrect label, as measured by the category corresponding to second most activated unit of the output layer of EfficientNet.<sup>1</sup> In the cases where EfficientNet incorrectly predicted the label, we used the wrong predicted label as the incorrect label. The final dataset contained 147 different images: 51 upright poses, 51 rotated-correct poses, and 45 rotated-incorrect poses (examples in Figure 1).<sup>2</sup>

The stimulus set applied here is not entirely ecologically realistic, as all objects are displayed without a background. However, our aim was to create a highly controlled stimulus set and experimental setup. Performance in canonical view is compared with performance with exactly the same object in a rotated view, both shown without background. Thus, any performance differences, be it human or network, can only be caused by rotation. Conversely, any robustness can

<sup>1</sup>In some cases, we had to choose the 3rd or the 4th best guess of EfficientNet, the criterion to discard the 2nd best guess being that it would be too similar to the correct label for a non-specialist human (e.g., golden retriever vs. labrador).

<sup>2</sup>There were fewer incorrectly identified poses, because in six cases, EfficientNet was able to correctly identify all 180 rotated poses.

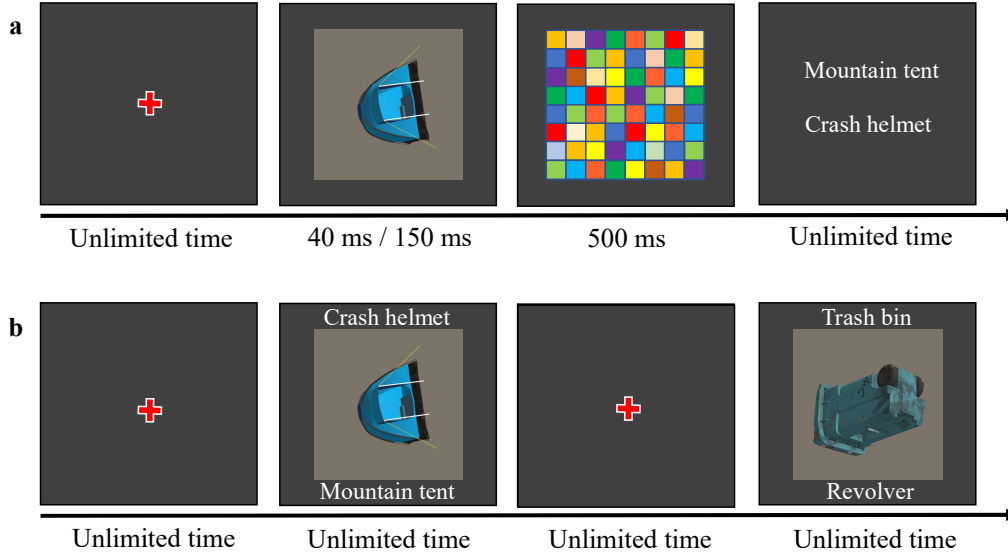


**Figure 2. Description of the human tests used in this study. a)** Task with limited viewing time: First the subject fixates on a cross, then an image is displayed for either 40 ms or 150 ms, followed by a dynamic checkerboard mask shown for 500 ms. Then the subject is asked to choose between two labels for the image (i.e., two-forced-choice task), and has an unlimited time to answer. **b)** Task with unlimited viewing time: similar test-setting, but now the image and the answer choices are displayed together for an unlimited viewing time and without back-masking.

only be caused by rotation-invariance, not context-based reasoning.

## 2.2. Psychophysics experiments

### 2.2.1. OBSERVERS

Altogether 24 observers (12 women, 12 men, aged 19-54) participated in the experiments. Our observers comprised Finnish students from diverse academic backgrounds, including disciplines such as engineering, psychology, business, and medicine. Participants were required to have normal vision or corrected-to-normal vision. Additionally, the observers did not report any medical condition (epilepsy, migraine, etc.) that could affect the results.

### 2.2.2. APPARATUS AND STIMULI

The object images were synthetic images of objects belonging to the ImageNet database classes. For information on the process of stimulus creation, see *Dataset collection 2.1* above. Noise masks, which were presented after object image presentation, consisted of dynamic white noise chromatic checkerboards (0.67 degrees of visual angle check size, 100 Hz temporal frequency). The diameter of the object images and the noise masks were 13.3 degrees of visual angle. The stimuli were presented using MATLAB Psychophysics Toolbox in a 22.5" VIEWPixx display with a resolution of 1200 x 1920 pixels, a frame rate of 100 Hz, and a viewing distance of 54 cm.

### 2.2.3. PROCEDURE

Prior to the experiments, observers were provided with a small training set, in order to familiarize themselves with the experimental procedure. None of the training objects were featured in the real experiment. After this training, each observer participated in a *limited viewing time* experiment and an *unlimited viewing time* experiment. In the *limited viewing time* experiment, each trial proceeded as follows (see Figure 2a). First, a fixation cross-hair was presented in the centre of the screen. Once the observer was ready, they pressed the space bar. After 500 ms, the object image was presented. The duration of the object image presentation was 40 ms for 12 observers, and 150 ms for the other 12. These stimulus durations (40 and 150 ms) were based on pilot experiments which suggested that those durations would lead to performance levels between perfect and chance level performance. The object image was immediately followed by 500 ms of dynamic chromatic white noise. After that, two response alternatives (in Finnish), one of them always the correct one, were presented and the observer had to choose (by pressing one of two keys on the keyboard) which alternative corresponded to the presented object. Each observer performed 49 trials, in which the image was in one of three types of poses: upright in 17 trials, rotated-correct (correctly classified by EfficientNet, see *Dataset collection 2.1*) in 17 trials, and rotated-incorrect (incorrectly classified by EfficientNet) in 15 trials. The trial types were interleaved and presented in random order. The *unlimited viewing time*

experiment (see Figure 2b) followed the same structure, except that the image remained on the screen until the observer responded (2.0 s on average), the labels were present from the start, and no noise was presented after the object image.

Each observer saw each object only in one pose during the limited viewing time experiment. The object-pose combinations were, however, balanced across observers such that each object was shown in a particular pose (e.g., upright) an equal amount of times. The order in which the objects were presented was different for every subject in order to avoid potential order effects. Furthermore, each observer saw exactly the same object-pose combinations they had seen in the limited time experiment for the unlimited time experiment. This allowed more powerful within-subject statistical analyses. In principle, the previous experience with the same images could affect the observers performance in the unlimited viewing time experiment. However, since the second presentation was not time-limited, making the task very easy for the viewer (see Results), we expect any advantage of having the image flashed previously to be negligible.

### 2.3. Machine tests

We implemented the same tests on a collection of 5 state-of-the-art deep networks for vision (referred below as 'pure vision networks') and 6 large vision-language models (VLM). Since EfficientNet was used to select the problematic images and labels, we did not include EfficientNet in this collection nor in our study of network robustness. We, in fact, investigated the *transfer* of errors between EfficientNet and these other networks.

We tested the 5 following pure vision networks: SWAG-RegNetY (Singh et al., 2022), BEiT-L/16 (Bao et al., 2021), ConvNext-XL (Liu et al., 2022), SWIN-L (Liu et al., 2021), and ViT-L/16 (Dosovitskiy et al., 2020) (see Appendix B for model descriptions). The network selection was based on previous work from Abbas & Deny (2023), which thoroughly evaluated the robustness of 37 state-of-the-art networks to objects presented in unusual poses. This collection provides a diverse set of state-of-the-art and very large models trained on large datasets (e.g., Imagenet-21K, Instagram 3.6B) with various architectures (ConvNet and Transformers) and training objectives (supervised and self-supervised). These networks obtained some of the most robust results to unusual poses according to Abbas & Deny (2023), and all of them were fine-tuned to the categories of ImageNet.

We mirrored the experiment done on humans by submitting each pure vision network to the same two-forced-choice test. Each network was shown the 147 different images of objects, 51 upright poses, 51 rotated-correct poses, and 45 rotated-incorrect poses. We compared the activations of the units of the final layer corresponding to each of the two categories given as choices for each image, and selected the

category with corresponding highest unit-activation among the two to be the chosen answer.

Our selection of VLMs included Gemini 1.5 Flash, Gemini 1.5 Pro, Claude 3 Opus, Claude 3.5 Sonnet, GPT-4o and GPT-4-vision-preview. The experiment was conducted via the API. Each model was shown the 147 images and provided with the following prompt (see examples in Appendix A):

*What's in this image?*

A. [label 1]

B. [label 2]

*Choose either A or B and answer in one or two words.*

If the model chose the correct label, the answer was counted as correct. If the model chose the wrong label or gave a response outside of the label options, the answer was counted as incorrect. If the model didn't provide any answer (e.g., Gemini threw a safety error for a few images), the image was disregarded and not included in the analysis.

### 2.4. Statistical tests

**T-tests:** We conducted a series of t-tests to compare the accuracies of different observers (networks and/or humans) and of the same observers in different viewing conditions (e.g., upright vs. rotated objects, limited vs. unlimited viewing time). When the data came from the same observers in two different viewing conditions, we used paired t-tests (i.e., 40 ms upright vs. 40 ms rotated) and unpaired t-tests when the observers were different (i.e., 40 ms rotated vs. 150 ms rotated). T-tests were run on percentages of correct answers.<sup>3</sup>

**Error consistency:** When two observers  $i$  and  $j$  (networks and/or humans) respond to the same  $n$  trials, we can measure how well their responses (correct/incorrect) align by computing their observed error overlap  $c_{obs_{i,j}}$ :

$$c_{obs_{i,j}} = \frac{e_{i,j}}{n}, \quad (1)$$

where  $e_{i,j}$  is the number of same responses, either both correct or incorrect. However, considering only the observed error overlap has limitations, because this overlap is expected to depend on overall accuracy of the observers in virtue of the probability of coincidence of two independent

<sup>3</sup>We acknowledge that %-accuracy is a non-linear index of performance and according to signal detection theory (Green et al., 1966), z-scores would be a more appropriate measure to use when computing means and performing statistical tests. However, since %-accuracy is more commonly used in the field of machine learning, we used %-accuracy when performing t-tests. We have, however, also conducted all our statistical tests with z-scores (not reported) and the changes in results were very minor, with no effect on the conclusions of this study.



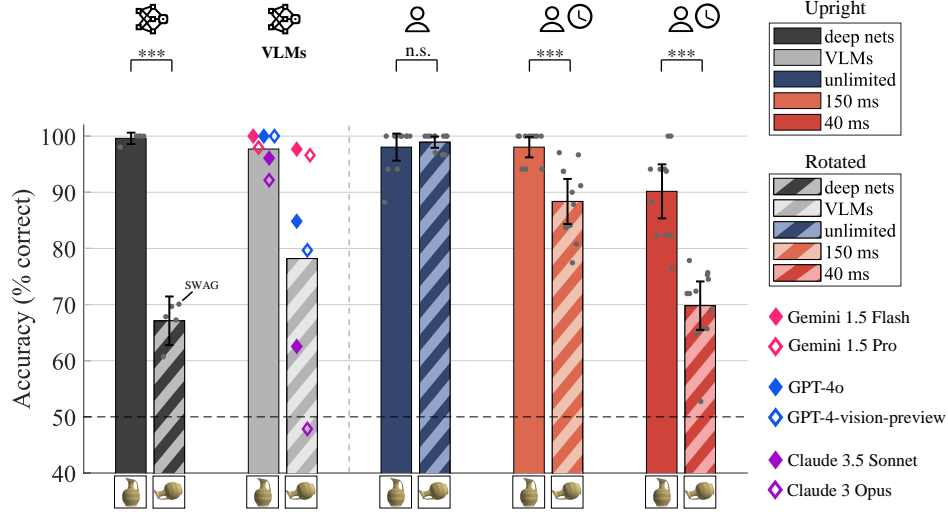


**Figure 3. Comparing neural networks and humans at recognizing objects in various poses.** Dark grey bars: Average performance of pure vision deep networks (left: upright vs. right: rotated) with 95% confidence intervals ( $n=5$ , grey points represent individual network performances). Light grey bars: Average performance of six large vision-language models (VLMs). Diamonds indicate individual model performances (full diamonds show the best-performing version of the different model classes). Blue bars: Average human performance with unlimited viewing time ( $n=12$ , grey points represent individual performances). Orange & Red bars: Average human performance with limited viewing time (150 ms and 40 ms, respectively,  $n=12$ , grey points represent individual performances). Chance performance is 50%. Three stars (\*\*\*) indicate highly significant differences ( $p < 0.001$ ), "n.s." for not significant. With unlimited time, humans excel at recognizing rotated objects, while pure vision networks struggle (best: SWAG at 70.1%). Both GPT-4 and Claude models follow the same pattern as the pure vision networks, with a significant drop in accuracy for rotated images compared to upright ones. However, Gemini 1.5 Flash mirrors human performance with unlimited viewing time, achieving 97.7% accuracy on rotated images compared to human accuracy of 98.9%. Limiting human viewing time (40 ms or 150 ms) impairs their ability to recognize rotated objects, substantially more than upright objects, bringing their performance closer to the network level.

binomial variables (e.g., a network and a human with 99% performance are expected to have more overlap than a network and human with 90% performance). To address this issue, we compare observers  $i$  and  $j$  to a theoretical model of independent binomial observers. This model considers two observers making random decisions, and thus we can only expect overlap due to chance. This expected error overlap  $c_{exp_{i,j}}$  is given by:

$$c_{exp_{i,j}} = p_i p_j + (1 - p_i)(1 - p_j), \quad (2)$$

where  $p_i p_j$  is the probability that observers give the same correct response by chance and  $(1 - p_i)(1 - p_j)$  the probability that they give the same incorrect response by chance. To evaluate the consistency between the two observers  $i$  and  $j$ , and determine whether it goes beyond what could be expected by chance, we use a metric called error consistency (Geirhos et al., 2020; 2021) (i.e., Cohen’s  $\kappa$ ) given by:

$$\kappa_{i,j} = \frac{c_{obs_{i,j}} - c_{exp_{i,j}}}{1 - c_{exp_{i,j}}}. \quad (3)$$

Error consistency compares observed consistency to expected consistency, and allows us to quantify whether the observed consistency is larger than would have been expected by chance.

### 3. Results

We compared human and machine vision on a task consisting in recognizing objects in unusual poses. For this, we selected 5 different pure vision deep neural networks (SWAG, ViT, SWIN, BEiT, ConvNext), chosen for their state-of-the-art performance in recognizing objects in unusual poses (Abbas & Deny, 2023), and 6 state-of-the-art large vision-language models (Gemini 1.5 Flash, Gemini 1.5 Pro, Claude 3 Opus, Claude 3.5 Sonnet, GPT-4o, GPT-4-vision-preview). We performed a two-alternative-forced-choice object categorization task: an image of an object was presented to the viewer (either deep network or human participant), and then the viewer had to choose between two different names (i.e., labels) for the object. The two labels were selected based on the highest activations of Noisy Student EfficientNet’s output layer (Xie et al., 2020), the most robust network to unusual poses according to Abbas & Deny (2023). For pure vision networks, the choice was made by looking at the highest activation of the softmax output layer for these two labels. EfficientNet was excluded from our analyses comparing humans and networks because images and labels were chosen based on its mistakes (see Methods). For the vision-language models, each VLM was

given an image and prompted with the 2 label choices, and the label chosen by the model was selected to be its answer. The performance of VLMs is discussed in the last paragraph of results, while previous paragraphs concentrate on the comparison of pure vision networks and humans.

**With unlimited viewing time, humans outperform deep networks at recognizing objects in unusual poses.** First, we compared the ability of humans and networks to recognize objects in upright and unusual poses when humans were not given any time limit for the object recognition (Figure 3). In the upright poses, both humans and neural networks performed very well: 4 networks obtained 100% accuracy and one (ViT-L) failed to correctly label only 1 out of 51 objects; humans had slightly lower performance with an accuracy of  $98.0\% \pm 2.4\%$  (95% confidence intervals). The very few errors that human observers made are likely to be keystroke errors and misunderstandings of the verbal response alternatives (as reported by some subjects). We conducted an additional test to discern whether network errors arise from changes in viewpoint, or alterations in image statistics between training and testing distributions (natural vs. synthetic). We subjected all five of our networks to a dataset comprising objects rotated at angles of  $\pm 10^\circ$  from their canonical poses. All of our networks obtained perfect or near-perfect results (SWAG-RegNetY: 100%, BEiT-L/16: 99.3%, ConvNext-XL: 98.2%, SWIN-L: 91.1%, ViT-L/16: 95.0%). *For unusual poses, human participants with unlimited viewing time clearly outperformed neural networks.* For humans, the performance on rotated images and upright images was on par (rotated condition:  $98.9\% \pm 1.0\%$ )( $t(11) = -0.79$ ,  $p = 0.45$ ), whereas for networks, the performance drastically dropped between upright ( $99.6\% \pm 1.0\%$ ) and rotated objects ( $67.1\% \pm 4.3\%$ ), with a drop of over 30% performance on average ( $t(4) = 18.7$ ,  $p = 4.8e-05$ ). Even the most robust network of our collection, SWAG trained on IG-3.6B (Singh et al., 2022), showed a drop in performance of 30% (from 100% on upright poses to 70.1% on rotated poses).

**Under limited viewing time, humans are faulty on unusual poses, like deep networks.** In the unlimited viewing time condition, observers used on average 2 seconds before taking a decision. We next studied the performance of human observers when the viewing time was limited to 40 ms and 150 ms followed by a dynamic white noise chromatic mask (Figure 3) (see Procedure 2.2.3 for the justification for these duration choices). With the upright poses, the accuracy of human observers decreased quite modestly (to  $90.2\% \pm 4.8\%$ ) when viewing time was 40 ms. The unlimited vs. 40 ms difference is statistically significant ( $t(22) = 3.19$ ,  $p = 0.0042$ ). The performance for 40 ms rotated images ( $69.8\% \pm 4.3\%$ ) drastically decreased compared to 40 ms upright images, with a drop of 20% ( $t(11) = 8.5$ ,  $p =$

$3.7e-06$ ). Additionally, the performance on 40 ms rotated images notably decreased compared to unlimited viewing time ( $98.9\% \pm 1.0\%$ )( $t(22) = 14.3$ ,  $p = 1.2e-12$ ). At 150 ms exposure time, performance was barely affected when the objects were presented upright ( $98.0\% \pm 1.8\%$  for the 150 ms viewing condition compared to  $98.0\% \pm 2.4\%$  for the unlimited viewing time condition). Subjects performed substantially better at recognizing objects in unusual poses when given 150 ms ( $88.4\% \pm 4.0\%$ ) compared to 40 ms ( $69.8\% \pm 4.3\%$ )( $t(22) = 6.9$ ,  $p = 6.7e-07$ ), but not as well as with unlimited viewing time ( $98.9\% \pm 1.0\%$ )( $t(11) = 7.0$ ,  $p = 2.3e-05$ ). We conclude that the process needed to recognize objects in unusual poses in the brain is impaired when interrupted by a mask after 40 ms viewing time, and starts taking place in a time frame of approximately 150 ms.

**Patterns of errors differ between humans and deep networks.** We next subdivided the unusual poses in two sets, the poses that EfficientNet predicted correctly (rotated-correct) vs. incorrectly (rotated-incorrect), and analysed the errors of humans and networks on these sets (Figure 4a). We found that errors made by EfficientNet transfer well to the 5 networks tested ( $80.0\% \pm 7.4$  accuracy on rotated-correct condition vs.  $54.2\% \pm 5.3$  on rotated-incorrect condition, a significant difference:  $t(4) = 6.99$ ,  $p = 0.0022$ )—despite the diversity of architectures and training procedures—but not to humans (difference in average performance between rotated-correct and rotated-incorrect non-significant). To investigate further whether networks and humans make similar errors (i.e., whether they classify incorrectly the same images), we computed error consistency (defined in Statistical tests 2.4) across networks, across humans, and between networks and humans. When computing the error consistency across networks and between humans and networks, we found that networks do similar mistakes to each other, but that human errors are on average not consistent with network errors (Figure 4b and c). Moreover, there is a greater diversity in the patterns of errors made by humans than in the pattern of errors made by networks. Overall, this suggests that the behavior of time-limited humans is different than the one of networks.

**We then sought to understand what qualitatively explained the differences in the error patterns between time-limited humans (40 ms) and deep networks.** We found that—even under acute time limitation—humans rely on different strategies than networks for recognition, relying more on object structure than their network counterparts (which rely on object details). In Figure 5a, we show examples where both networks and humans performed well. In these examples, both the structure and details of the objects are well informative about the identity of the object. In Figure 5b, we show examples of errors that networks made but humans typically didn't. A striking example is the image of

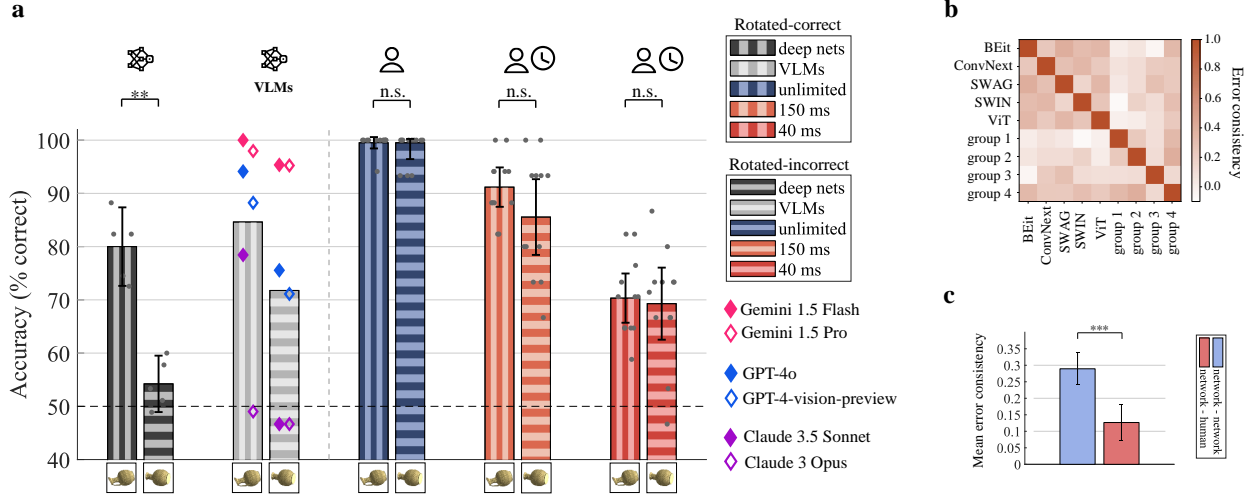


**Figure 4. Error patterns are different for neural networks and time-limited humans.** **a)** Comparison of human and network accuracy for the rotated-correct condition (EfficientNet was correct on these rotations) vs. rotated-incorrect condition (rotations that have failed EfficientNet). Humans show consistent accuracy between rotated-correct and rotated-incorrect conditions. In contrast, networks, including the six VLMs (represented by diamonds), exhibit a performance drop. However, for Gemini 1.5 Flash, Gemini 1.5 Pro and Claude Opus, the decrease in performance between the two conditions is not as notable. **b)** Error consistency analysis performed on the 5 neural networks (not including VLMs) and 40 ms time-limited human subjects. 12 human subjects were partitioned into 4 groups of 3, so that every group saw each rotated image exactly once. The darker red cluster for networks (dark red = highly consistent errors) indicates that they have similar patterns of error, which are not shared by human subjects, highlighting that EfficientNet errors transfer better to other networks than to humans. **c)** Mean error consistencies were calculated by comparing networks with each other and with human subjects (i.e., average computed over the different matrix clusters). A two-tailed unpaired t-test confirms that networks indeed make more consistent errors with each other than with humans ( $t(28) = 4.0$ ,  $p = 3.8e-04$ ).

a stretcher, which networks mislabeled as a matchstick. We speculate that the similarity between the stretcher’s legs and matchsticks is the cause for this misclassification. Despite the resemblance to matchsticks, humans however correctly identified the object because the overall structure of the object rules out the possibility of matchsticks. Thus, we can reason that in that case, humans tended to perceive the overall structure rather than fixating on minute details, unlike networks which based their prediction on such details. In Figure 5c, we show examples where identification of an object is challenging for humans but not for networks. For instance, images of jellyfish posed difficulties for human observers. The shortness of the exposure time, 40 ms, could potentially limit humans to recognising only the overall shape and color of the object, compatible with both a lampshade and a jellyfish. In contrast, networks are able to process fine details, such as the patterns on the jellyfish’s umbrella, allowing for accurate identification regardless of pose. Figure 5d presents examples that prove to be challenging for both humans and networks. It can be noted that in all these examples, both the structure and details contain only limited information about the object identity. The impairment of both networks and humans on these images is thus consistent with our hypothesis that humans rely on structure and networks on details for recognition. These qualitative

observations reinforce our conclusion that time-limited humans are not well-modelled by feed-forward networks.

**Next, we tested six large vision-language models (VLMs): GPT-4o, GPT-4-vision-preview, Claude 3.5 Sonnet, Claude 3 Opus, Gemini 1.5 Flash and Gemini 1.5 Pro.** With upright poses, all 6 models performed well (Gemini 1.5 Flash, GPT-4o and GPT-4-vision-preview achieving 100% accuracy, Gemini 1.5 Pro 98.0%, Claude 3.5 Sonnet 94.1% and Claude 3 Opus 92.2%). However, there were significant differences in performance when recognizing rotated poses (Figure 3). Claude 3 Opus performed below the 50% chance level, achieving only 45.8% accuracy. Claude 3.5 Sonnet’s accuracy was on par with pure vision networks with 62.5% accuracy. GPT-4o had an accuracy of 84.8% and GPT-4-vision-preview 79.7%, performing substantially better than our best performing pure vision model, SWAG (70.1%). Remarkably, Gemini 1.5 Pro achieved an accuracy of 96.6% and Gemini 1.5 Flash an accuracy of 97.7%, performances on par with unlimited humans (98.9%). Separating the rotated condition into two categories—rotated-correct (images correctly labelled by EfficientNet) and rotated-incorrect (images incorrectly labelled by EfficientNet)—revealed that the 6 VLMs exhibited a performance drop between these conditions, similarly to the five pure vision networks (Figure 4a).

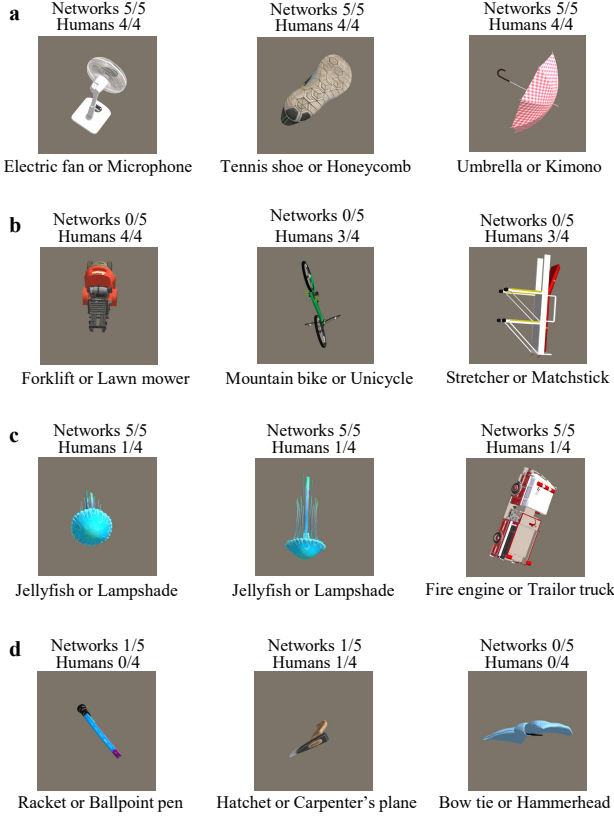


**Figure 5. Examples of objects in unusual poses, where deep networks for pure vision and 40 ms time-limited humans made similar and differing errors.** Above each image is a quantitative score of correct answers and below each image are the given answer choices, correct answer being the first. **a)** Images where all networks and humans correctly labeled the object. **b)** Images where all networks failed to correctly label the objects, but where humans mostly chose the correct answer. **c)** Images, where all the networks correctly labeled the objects, but where most humans failed. **d)** Images, where both networks and humans were mostly not able to correctly label the object.

Performance differences of GPT-4o (18%), GPT-4-vision-preview (17%) and Claude 3.5 Sonnet (32%) were the most similar to the 5 pure vision networks, whose average performance gap was 26%. For Gemini models and Claude 3 Opus, the performance differences were much smaller: 4.7% for Gemini 1.5 Flash, 2.7% for Gemini 1.5 Pro and 2.4% for Claude. For both unlimited and time-limited humans, the performance difference was not significant between the two conditions. This suggests that errors from EfficientNet transfer better to most VLMs than to humans.

## 4. Discussion

Our results strikingly demonstrate that the human visual system is more robust than deep networks for vision and than most vision-language models at recognizing objects in

unusual poses. Indeed, with unlimited viewing time, human performance is not affected by unusual poses, whereas deep networks are fooled by them. Only in the very limited viewing time condition (40 ms) does the performance of humans deteriorate to the level of deep networks.

### 4.1. The gap still exists

Our finding is in contrast to a recent study (Geirhos et al., 2021) which showed that deep networks are closing the performance gap with humans on many out-of-distribution visual tasks. Our study differs from this recent study in two major ways: (1) We are considering a transformation (object pose) which affects the global structure of the image, unlike the distortions studied in (Geirhos et al., 2021) which mostly affected the local texture of images (e.g., blur, color modifications, stylization); (2) Geirhos et al. (2021) compare network performance to time-limited humans only. The human subjects in their study were given 200 ms to view the image, followed by a mask. We find that viewing time does affect the robustness of recognition in a crucial way. When time-limited to 40 ms or 150 ms (followed by a mask), the performance of humans substantially degrades at recognizing objects in unusual poses.

Regarding the deep networks, it is notable that the architecture (e.g., visual transformers vs. convolutional neural networks), loss function (e.g., self-supervised vs. supervised), training set size (e.g., 3.6 billion images for SWAG) and modality (pure images, or images and text) did not affect their performance on the task (with the exception of Gemini, see discussion below). This observation adds to a literature showing that scaling alone seems insufficient to match human internal representations and performance in visual tasks (e.g., (Shankar et al., 2020; Fel et al., 2022; Mutenthaler et al., 2022; Linsley et al., 2023a;b)). We also note that networks do not benefit from additional time, as their processing time is fixed by the nature of their feed-forward architecture.

### 4.2. Why do humans need the extra time?

Our results are in line with a tradition of psychology studies (Shepard & Metzler, 1971; Jolicoeur, 1985; Edelman & Bülthoff, 1992; Kosslyn et al., 1994; Sofer et al., 2015; Jeurissen et al., 2016; Kallmayer et al., 2023; Mayo et al., 2024) showing that humans need more time to accomplish more challenging visual tasks. Closest to our work, Jolicoeur (1985) showed that the naming time of sketches of everyday objects was proportional to the difference in orientation with their upright pose. Below, we list some of the possible mental processes that could be responsible for this extra time:

**1) Evidence accumulation:** The increased time could



be needed for evidence accumulation. For example, it is known that different types of information about a visual stimulus (e.g., coarse vs. fine features, low contrast vs. high contrast features) propagate to cortical visual areas with different timings (Van Rullen & Thorpe, 2001; VanRullen & Thorpe, 2002). It might thus be necessary to see the stimulus for a certain time for all relevant information to arrive to cortex. Additionally, stimulus information always involves a certain amount of noise and uncertainty, which can be filtered with increased viewing time (Olds & Engel, 1998; Perrett et al., 1998).

**2) Recurrence within the visual system:** The visual system is known to be highly recurrent (Felleman & Van Essen, 1991; Suzuki et al., 2023). Previous evidence suggests that visual information is mainly processed in a feed-forward way during the first 80 ms after exposure (Liu et al., 2009; Wyatte et al., 2014; Cichy et al., 2016; Mohsenzadeh et al., 2018), after which recurrent processes start taking place within the visual system (Liu et al., 2009; Thorpe, 2009; Wyatte et al., 2014; Cichy et al., 2016; Kar & DiCarlo, 2021), e.g., from extrastriate areas to V1. Moreover, other studies have suggested that backward masks, such as the ones used in this study, disrupt these recurrent processes (Lamme & Roelfsema, 2000; Lamme et al., 2002; Breitmeyer & Ogmen, 2006; Fahrenfort et al., 2007; Macknik & Martinez-Conde, 2007). The observed drop in human performance from 150 ms to 40 ms viewing time could thus be explained by these recurrent processes taking place in the 150 ms condition but being interrupted by backward masking in the 40 ms condition. From a computational standpoint, there is mounting evidence that these recurrent circuits provide important functions such as grouping and filling-in of features, and are important for object identification in noisy real-world situations, and particularly when objects are partially occluded (Wyatte et al., 2014). It is an interesting possibility that incorporating such recurrence in deep networks could bring human-like robustness to recognition of objects in unusual poses. Some efforts to incorporate recurrence in deep learning models of the visual system exist (Wyatte et al., 2012; O'Reilly et al., 2013; Spoerer et al., 2017; Tang et al., 2018; Kietzmann et al., 2019; Rajaei et al., 2019; Nayeibi et al., 2022; Goetschalckx et al., 2023), but to our knowledge not in the context of recognizing objects in unusual poses.

We note that evidence accumulation and recurrence are not mutually exclusive and, in fact, recurrent circuits are one possible neural implementation to allow evidence accumulation.

**3) Recurrence between the visual system and other systems:** The neural substrate is also highly recurrent be-

tween the visual system and other brain regions (Felleman & Van Essen, 1991), such as the perirhinal cortex in the medial temporal lobe (Bonnen et al., 2023) and many frontoparietal areas, such as the prefrontal cortex (PFC) and the Frontal Eye Fields (FEF). Feedback processes originating in frontoparietal areas through reciprocal connections to striate cortex provide attentional support to salient or behaviorally-relevant features (Wyatte et al., 2014). FEF, in turn, play a crucial role in the initiation and execution of saccadic eye movements. The additional processing time could be needed to perform saccades across the object to encode the objects' subparts with successive fixations. Medial temporal cortex (MTC) has been recently shown to support object perception by integrating over multiple glances or saccades (Bonnen et al., 2023). However, these recurrent interactions between the visual systems and other areas are thought to take place at least 150 ms after the first glance (Wyatte et al., 2014; Bonnen et al., 2023). They can only partly explain the performance for unusual poses we observe, since we already see a great improvement from 40 ms to 150 ms, before these interactions could take place.

#### 4.3. Time-limited humans are not feed-forward deep networks

Both time-limited humans and networks have similar error rates at recognizing objects in unusual poses. This result could suggest that time-limited humans are well-modelled by feed-forward deep networks, as proposed by (Yamins et al., 2014; Rajalingham et al., 2018; Kar et al., 2019; Serre, 2019; Dapello et al., 2020; Kar & DiCarlo, 2021; Dapello et al., 2022; Muttenthaler et al., 2022; Bonnen et al., 2023; Dehghani et al., 2023). Here, our analysis of the error patterns of time-limited humans vs. networks suggests otherwise. While the performance of networks and time-limited humans is similar on unusual poses, there is little consistency in their patterns of error. Networks share consistent patterns of error with each other, which are inconsistent with the patterns of error of humans. In addition, humans are overall more unpredictable in their error patterns than networks. Moreover, a qualitative analysis of the problematic images for networks vs. humans suggests that networks make errors when they overlook the overall structure of the object and rely instead on misleading details or textures. Conversely, time-limited humans tend to make errors when the overall structure of the object is not clearly disambiguating the object identity, and where one should instead rely on details of the object and textures to make the correct decision. This discrepancy is in line with previous studies (Geirhos et al., 2018; Rajalingham et al., 2018; Geirhos et al., 2021; Wichmann & Geirhos, 2023) which have shown that deep networks do not make the same mistakes as time-limited humans. In particular, Geirhos et al. (2018) showed that deep networks are prone to a bias

towards texture, whereas humans are prone to a bias towards shape of objects in their perceptual decisions. Our results suggest that this discrepancy persists under extreme time limitation, and that feed-forward deep networks are not adequate models of time-limited humans.

#### 4.4. On the role of retrospective thinking in humans and vision-language models

In the current study, humans were presented with an image followed by a two-alternative-forced-choice question. This provides humans with an opportunity to utilize retrospective thinking. For instance, a subject who initially failed to identify an image of a rotated stretcher, could reconsider their interpretation after seeing the answer alternatives 'stretcher' and 'matchstick'. Deep networks for pure vision, on the other hand, are not capable of such retrospective thinking; they classify the object based on the predefined 1000 classes without the possibility of a retrospective thought process when given the two possible answers. Conversely, large vision-language models are given the opportunity to ponder the content of the image after being fed the two labels, like humans. Their performance is notably better than deep networks for pure vision (except Claude), and even matching human performance in the case of Gemini. The impressive performance of vision-language models suggests that they might be able to exploit similar mechanisms for image recognition as humans, which could for instance involve retro-fitting the labels to the image. However, an alternative explanation is that they could have been fed a different data diet involving more rotated objects than their pure vision counterparts. Because of the limited documentation available for these models, it is difficult to come to a firm conclusion regarding the mechanisms underlying their abilities.

#### Acknowledgements

This work has been supported by an Aalto Brain Center (ABC) grant to N.O., and an Academy of Finland (AoF) grant to S.D. under the AoF Project: 3357590.

#### Impact Statement

Deep learning-based computer vision systems are nowadays used in applications where robustness is critical, such as automated vehicle driving. It is thus important to document the robustness of these systems even in rare conditions, for example here when objects are presented in unusual poses. The comparison to human vision is interesting to assess whether the computer vision systems are reaching the robustness of humans, and can lead to insights to understand how the human visual system works.

#### References

- Abbas, A. and Deny, S. Progress and limitations of deep networks to recognize objects in unusual poses. *AAAI*, 2023.
- Alcorn, M. A., Li, Q., Gong, Z., Wang, C., Mai, L., Ku, W.-S., and Nguyen, A. Strike (with) a pose: Neural networks are easily fooled by strange poses of familiar objects. In *Proceedings of the IEEE/CVF Conference on Computer Vision and Pattern Recognition*, 2019.
- Bao, H., Dong, L., and Wei, F. Beit: Bert pre-training of image transformers. *arXiv preprint arXiv:2106.08254*, 2021.
- Bonnen, T., Wagner, A. D., and Yamins, D. L. Medial temporal cortex supports compositional visual inferences. *bioRxiv*, 2023.
- Breitmeyer, B. and Ogmen, H. *Visual masking: Time slices through conscious and unconscious vision*. 2006.
- Cichy, R. M., Pantazis, D., and Oliva, A. Similarity-based fusion of meg and fmri reveals spatio-temporal dynamics in human cortex during visual object recognition. *Cerebral Cortex*, 2016.
- Cubuk, E. D., Zoph, B., Shlens, J., and Le, Q. V. Randaugment: Practical automated data augmentation with a reduced search space. In *Proceedings of the IEEE/CVF conference on computer vision and pattern recognition workshops*, 2020.
- Dapello, J., Marques, T., Schrimpf, M., Geiger, F., Cox, D., and DiCarlo, J. J. Simulating a primary visual cortex at the front of cnns improves robustness to image perturbations. *Advances in Neural Information Processing Systems*, 2020.
- Dapello, J., Kar, K., Schrimpf, M., Geary, R., Ferguson, M., Cox, D. D., and DiCarlo, J. J. Aligning model and macaque inferior temporal cortex representations improves model-to-human behavioral alignment and adversarial robustness. *bioRxiv*, 2022.
- Dehghani, M., Djolonga, J., Mustafa, B., Padlewski, P., Heek, J., Gilmer, J., Steiner, A. P., Caron, M., Geirhos, R., Alabdulmohsin, I., Jenatton, R., Beyer, L., Tschannen, M., Arnab, A., Wang, X., Riquelme Ruiz, C., Minderer, M., Puigcerver, J., Evci, U., Kumar, M., Steenkiste, S. V., Elsayed, G. F., Mahendran, A., Yu, F., Oliver, A., Huot, F., Bastings, J., Collier, M., Gritsenko, A. A., Birodkar, V., Vasconcelos, C. N., Tay, Y., Mensink, T., Kolesnikov, A., Pavetic, F., Tran, D., Kipf, T., Lucic, M., Zhai, X., Keysers, D., Harmsen, J. J., and Houlsby, N. Scaling vision transformers to 22 billion parameters. *Proceedings of the 40th International Conference on Machine Learning*, 2023.

- Devlin, J., Chang, M.-W., Lee, K., and Toutanova, K. Bert: Pre-training of deep bidirectional transformers for language understanding. *arXiv preprint arXiv:1810.04805*, 2018.
- Dosovitskiy, A., Beyer, L., Kolesnikov, A., Weissenborn, D., Zhai, X., Unterthiner, T., Dehghani, M., Minderer, M., Heigold, G., Gelly, S., et al. An image is worth 16x16 words: Transformers for image recognition at scale. *arXiv preprint arXiv:2010.11929*, 2020.
- Edelman, S. and Bülthoff, H. H. Orientation dependence in the recognition of familiar and novel views of three-dimensional objects. *Vision research*, 1992.
- Fahrenfort, J. J., Scholte, H. S., and Lamme, V. A. Masking disrupts reentrant processing in human visual cortex. *Journal of cognitive neuroscience*, 2007.
- Fel, T., Rodriguez Rodriguez, I. F., Linsley, D., and Serre, T. Harmonizing the object recognition strategies of deep neural networks with humans. *Advances in Neural Information Processing Systems*, 2022.
- Felleman, D. J. and Van Essen, D. C. Distributed hierarchical processing in the primate cerebral cortex. *Cerebral cortex (New York, NY: 1991)*, 1991.
- Geirhos, R., Rubisch, P., Michaelis, C., Bethge, M., Wichmann, F. A., and Brendel, W. Imagenet-trained cnns are biased towards texture; increasing shape bias improves accuracy and robustness. *arXiv preprint arXiv:1811.12231*, 2018.
- Geirhos, R., Meding, K., and Wichmann, F. A. Beyond accuracy: quantifying trial-by-trial behaviour of cnns and humans by measuring error consistency. *Advances in Neural Information Processing Systems*, 2020.
- Geirhos, R., Narayanappa, K., Mitzkus, B., Thieringer, T., Bethge, M., Wichmann, F. A., and Brendel, W. Partial success in closing the gap between human and machine vision. *arXiv preprint arXiv:2106.07411*, 2021.
- Goetschalckx, L., Govindarajan, L. N., Ashok, A. K., Ahuja, A., Sheinberg, D. L., and Serre, T. Computing a human-like reaction time metric from stable recurrent vision models. *arXiv:2306.11582*, 2023.
- Green, D. M., Swets, J. A., et al. *Signal detection theory and psychophysics*. 1966.
- He, K., Zhang, X., Ren, S., and Sun, J. Delving deep into rectifiers: Surpassing human-level performance on imagenet classification. *Proceedings of the IEEE International Conference on Computer Vision (ICCV)*, 2015.
- Ibrahim, M., Garrido, Q., Morcos, A., and Bouchacourt, D. The robustness limits of sota vision models to natural variation. *arXiv preprint arXiv:2210.13604*, 2022.
- Jeurissen, D., Self, M. W., and Roelfsema, P. R. Serial grouping of 2d-image regions with object-based attention in humans. *eLife*, 2016.
- Jolicoeur, P. The time to name disoriented natural objects. *Memory & Cognition*, 1985.
- Kallmayer, A., Vö, M. L.-H., and Draschkow, D. View-point dependence and scene context effects generalize to depth rotated three-dimensional objects. *Journal of Vision*, 2023.
- Kar, K. and DiCarlo, J. J. Fast recurrent processing via ventrolateral prefrontal cortex is needed by the primate ventral stream for robust core visual object recognition. *Neuron*, 2021.
- Kar, K., Kubilius, J., Schmidt, K., Issa, E. B., and DiCarlo, J. J. Evidence that recurrent circuits are critical to the ventral stream’s execution of core object recognition behavior. *Nature Neuroscience*, 2019.
- Kietzmann, T. C., Spoerer, C. J., Sörensen, L. K., Cichy, R. M., Hauk, O., and Kriegeskorte, N. Recurrence is required to capture the representational dynamics of the human visual system. *Proceedings of the National Academy of Sciences*, 2019.
- Kosslyn, S. M., Alpert, N. M., Thompson, W. L., Chabris, C. F., Rauch, S. L., and Anderson, A. K. Identifying objects seen from different viewpoints a pet investigation. *Brain*, 1994.
- Lamme, V. and Roelfsema, P. The distinct modes of vision offered by feedforward and recurrent processing. *Trends in neurosciences*, 2000.
- Lamme, V. A., Zipser, K., and Spekreijse, H. Masking interrupts figure-ground signals in v1. *Journal of cognitive neuroscience*, 2002.
- Linsley, D., Feng, P., Boissin, T., Ashok, A. K., Fel, T., Olaiya, S., and Serre, T. Adversarial alignment: Breaking the trade-off between the strength of an attack and its relevance to human perception. *arXiv preprint arXiv:2306.03229*, 2023a.
- Linsley, D., Rodriguez, I. F., Fel, T., Arcaro, M., Sharma, S., Livingstone, M., and Serre, T. Performance-optimized deep neural networks are evolving into worse models of inferotemporal visual cortex. *arXiv preprint arXiv:2306.03779*, 2023b.

- Liu, H., Agam, Y., Madsen, J. R., and Kreiman, G. Timing, timing, timing: fast decoding of object information from intracranial field potentials in human visual cortex. *Neuron*, 2009.
- Liu, Z., Lin, Y., Cao, Y., Hu, H., Wei, Y., Zhang, Z., Lin, S., and Guo, B. Swin transformer: Hierarchical vision transformer using shifted windows. In *Proceedings of the IEEE/CVF International Conference on Computer Vision*, pp. 10012–10022, 2021.
- Liu, Z., Mao, H., Wu, C.-Y., Feichtenhofer, C., Darrell, T., and Xie, S. A convnet for the 2020s. *arXiv preprint arXiv:2201.03545*, 2022.
- Macknik, S. L. and Martinez-Conde, S. The role of feedback in visual masking and visual processing. *Advances in cognitive psychology*, 2007.
- Madan, S., Sasaki, T., Pfister, H., Li, T.-M., and Boix, X. Adversarial examples within the training distribution: A widespread challenge. *arXiv preprint arXiv:2106.16198*, 2021.
- Madan, S., Henry, T., Dozier, J., Ho, H., Bhandari, N., Sasaki, T., Durand, F., Pfister, H., and Boix, X. When and how convolutional neural networks generalize to out-of-distribution category–viewpoint combinations. *Nature Machine Intelligence*, 2022.
- Mayo, D., Cummings, J., Lin, X., Gutfreund, D., Katz, B., and Barbu, A. How hard are computer vision datasets? calibrating dataset difficulty to viewing time. *Advances in Neural Information Processing Systems*, 2024.
- Mohsenzadeh, Y., Qin, S., Cichy, R. M., and Pantazis, D. Ultra-rapid serial visual presentation reveals dynamics of feedforward and feedback processes in the ventral visual pathway. *Elife*, 2018.
- Muttenthaler, L., Dippel, J., Linhardt, L., Vandermeulen, R. A., and Kornblith, S. Human alignment of neural network representations. *arXiv preprint arXiv:2211.01201*, 2022.
- Nayebi, A., Sagastuy-Brena, J., Bear, D. M., Kar, K., Kubilius, J., Ganguli, S., Sussillo, D., DiCarlo, J. J., and Yamins, D. L. K. Recurrent connections in the primate ventral visual stream mediate a trade-off between task performance and network size during core object recognition. *Neural Computation*, 2022.
- Olds, E. S. and Engel, S. A. Linearity across spatial frequency in object recognition. *Vision Research*, 1998.
- O’Reilly, R. C., Wyatte, D., Herd, S., Mingus, B., and Jilk, D. J. Recurrent processing during object recognition. *Frontiers in psychology*, 2013.
- Perrett, D., Oram, M., and Ashbridge, E. Evidence accumulation in cell populations responsive to faces: an account of generalisation of recognition without mental transformations. *Cognition*, 1998.
- Rajaei, K., Mohsenzadeh, Y., Ebrahimpour, R., and Khaligh-Razavi, S.-M. Beyond core object recognition: Recurrent processes account for object recognition under occlusion. *PLoS Comput Biol*, 2019.
- Rajalingham, R., Issa, E. B., Bashivan, P., Kar, K., Schmidt, K., and DiCarlo, J. J. Large-scale, high-resolution comparison of the core visual object recognition behavior of humans, monkeys, and state-of-the-art deep artificial neural networks. *Journal of Neuroscience*, 2018.
- Serre, T. Deep learning: the good, the bad, and the ugly. *Annual review of vision science*, 2019.
- Shankar, V., Roelofs, R., Mania, H., Fang, A., Recht, B., and Schmidt, L. Evaluating machine accuracy on imagenet. In *International Conference on Machine Learning*, 2020.
- Shepard, R. N. and Metzler, J. Mental rotation of three-dimensional objects. *American Assn for the Advancement of Science*, 1971.
- Singh, M., Gustafson, L., Adcock, A., de Freitas Reis, V., Gedik, B., Kosaraju, R. P., Mahajan, D., Girshick, R., Dollár, P., and van der Maaten, L. Revisiting weakly supervised pre-training of visual perception models. In *Proceedings of the IEEE/CVF Conference on Computer Vision and Pattern Recognition*, 2022.
- Sofer, I., Crouzet, S. M., and Serre, T. Explaining the timing of natural scene understanding with a computational model of perceptual categorization. *PLoS Comput Biol*, 2015.
- Spoerer, C. J., McClure, P., and Kriegeskorte, N. Recurrent convolutional neural networks: a better model of biological object recognition. *Frontiers in psychology*, 2017.
- Suzuki, M., Pennartz, C. M., and Aru, J. How deep is the brain? the shallow brain hypothesis. *Nature Reviews Neuroscience*, 2023.
- Tang, H., Schrimpf, M., Lotter, W., Moerman, C., Paredes, A., Ortega Caro, J., Hardesty, W., Cox, D., and Kreiman, G. Recurrent computations for visual pattern completion. *Proceedings of the National Academy of Sciences*, 2018.
- Thorpe, S. J. The speed of categorization in the human visual system. *Neuron*, 2009.
- Van Rullen, R. and Thorpe, S. J. Rate coding versus temporal order coding: what the retinal ganglion cells tell the visual cortex. *Neural computation*, 2001.



- VanRullen, R. and Thorpe, S. J. Surfing a spike wave down the ventral stream. *Vision research*, 2002.
- Vasudevan, V., Caine, B., Gontijo Lopes, R., Fridovich-Keil, S., and Roelofs, R. When does dough become a bagel? analyzing the remaining mistakes on imagenet. *Advances in Neural Information Processing Systems*, 2022.
- Wichmann, F. A. and Geirhos, R. Are deep neural networks adequate behavioral models of human visual perception? *Annual Review of Vision Science*, 2023.
- Wyatte, D., Curran, T., and O'Reilly, R. The limits of feed-forward vision: Recurrent processing promotes robust object recognition when objects are degraded. *Journal of Cognitive Neuroscience*, 2012.
- Wyatte, D., Jilk, D. J., and O'Reilly, R. C. Early recurrent feedback facilitates visual object recognition under challenging conditions. *Frontiers in psychology*, 2014.
- Xie, Q., Luong, M.-T., Hovy, E., and Le, Q. V. Self-training with noisy student improves imagenet classification. In *Proceedings of the IEEE/CVF conference on computer vision and pattern recognition*, 2020.
- Yamins, D. L., Hong, H., Cadieu, C. F., Solomon, E. A., Seibert, D., and DiCarlo, J. J. Performance-optimized hierarchical models predict neural responses in higher visual cortex. *Proceedings of the national academy of sciences*, 2014.
- Zeng, X., Liu, C., Wang, Y.-S., Qiu, W., Xie, L., Tai, Y.-W., Tang, C.-K., and Yuille, A. L. Adversarial attacks beyond the image space. In *Proceedings of the IEEE/CVF Conference on Computer Vision and Pattern Recognition*, 2019.

## Appendix

### A. Testing Large Vision-Language Models

We tested 6 large vision-language models, Gemini 1.5 Flash, Gemini 1.5 Pro, GPT-4o, GPT-4-vision-preview, Claude 3.5 Sonnet and Claude 3 Opus, via their API. Figure 6 shows an example of the used prompt and models’ answers.

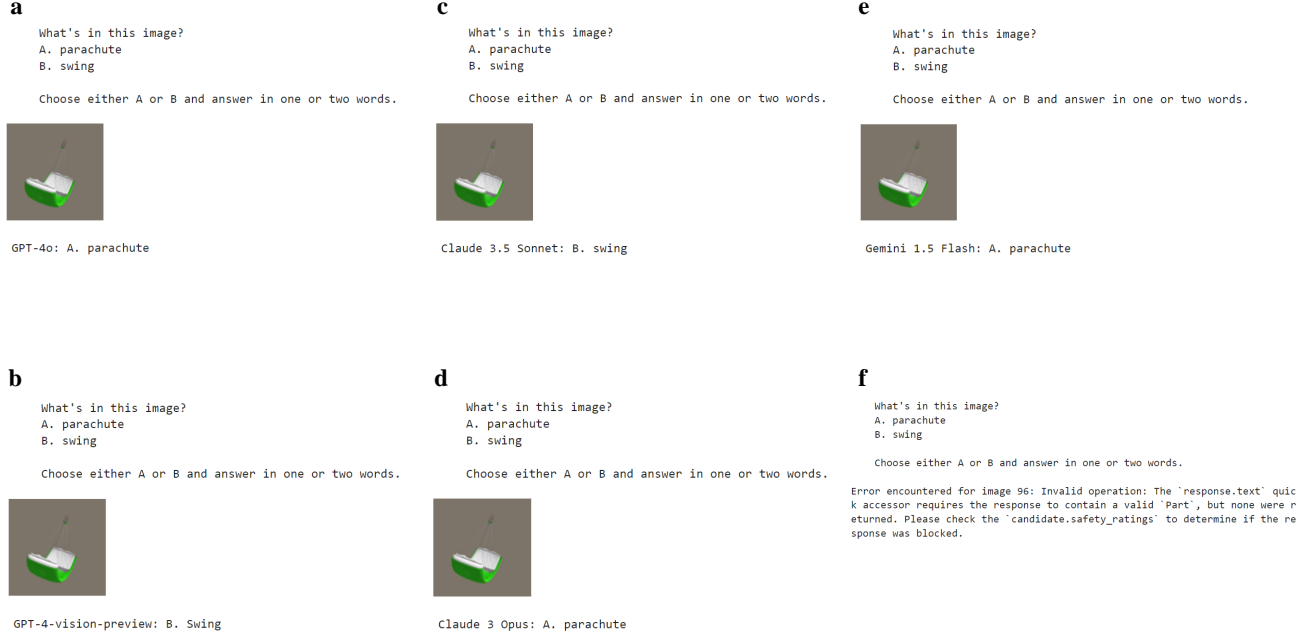


Figure 6. Examples of a prompt and models’ answers in API mode. a) GPT-4o, b) GPT-4-vision-preview, c) Claude 3.5 Sonnet, d) Claude 3 Opus, e) Gemini 1.5 Flash and f) Gemini 1.5 Pro (example of safety-blocked instance, which was disregarded in our analysis).

### B. Deep Networks (pure vision) details

#### B.1. Dataset and Training Objectives

We used six different models in this experiment: Noisy Student EfficientNet-L2, SWAG-RegNetY, ViT-L16, BEiT-L/16, ConvNeXt-XL, and SWIN-L. The models were chosen for their demonstrated performance at recognizing objects in unusual poses in a prior study conducted by (Abbas & Deny, 2023). The models were trained on datasets of varying sizes ranging from 1 million (ImageNet) to 3.6 billion images (IG-3.6B). These models had a variety of architectures (e.g., convolutional architecture, visual transformer) and were trained under a variety of training objectives:

- Supervised learning: Visual Transformers (Dosovitskiy et al., 2020; Liu et al., 2021) and convolutional architectures (Liu et al., 2022).
- Self-supervised learning: BEiT (Bao et al., 2021).
- Semi-supervised learning: Noisy Student (Xie et al., 2020).
- Semi-weakly supervised learning: SWAG (Singh et al., 2022).

#### B.2. Model Descriptions

This section describes the networks used in this study in detail.

**Standard Vision Transformer:** Standard Vision Transformer ViT-L/16 (Dosovitskiy et al., 2020) which was pretrained on ImageNet(1M) with input size 224x224.

**BEiT:** BEiT-L/16 is a Vision Transformer trained using a self-supervised training method introduced with the model (Bao et al., 2021). The method is known as Masked Image Modeling (MIM) and it is inspired by Masked Language Modeling (MLM) (Devlin et al., 2018). The model is pretrained with the self-supervised MIM task on ImageNet21k(14M) and fine-tuned on ImageNet. Even with smaller pretraining datasets, BEiT outperforms standard Visual Transformers.

**ConvNext:** ConvNeXt-XL (Liu et al., 2022), is a pure convolutional architecture which layers are designed carefully by choosing an optimal collection of architecture hyperparameters. The model undergoes training methods established for Visual Transformers, and they are known to enhance ConvNext’s performance as well. The model is trained on ImageNet21k(14M).

**SWIN Transformer:** SWIN-L Transformer (Liu et al., 2021) is a hierarchical Vision Transformer. The self-attention layer of the original Vision Transformer is replaced by a Shifted Window Self-attention layer (SWSA). The SWSA layer divides the image into windows, calculating self-attention within each window. This process significantly reduces the computational time of the attention layer, making it linear with the input size instead of quadratic. Additionally, it enhances performance compared to the original Visual Transformers. The model is trained on ImageNet21K(14M).

**Noisy Student:** Noisy Student EfficientNet-L2 is pretrained using the Noisy Student paradigm (Xie et al., 2020). The model is trained on ImageNet dataset and on the noisily labeled JFT-300M dataset. It has an input size of 475x475. The model is pretrained with the data augmentation method RandAugment (Cubuk et al., 2020), which among other distortions produces rotated images of the training set.

**SWAG:** SWAG-RegNetY (Singh et al., 2022) is pretrained using a semi-weakly supervised pretraining procedure. The pretraining dataset consisted of more than 3.6 billion Instagram images, which were labeled with hashtags of 27K classes.

### B.3. Model Sources

The checkpoints for all the models we use are in PyTorch format. The models are from three different main sources: Pytorch Image Model library (timm) (ViT-L16, ConvNext-XL, SWIN-L), Hugging Face Transformers library (BEiT-L16), and Torch Hub (EffN-L2-NS, SWAG-RegNetY).

## C. The 3D objects

Below are the 3D objects used in our experiments. They are listed with the links to Sketchfab. Images of each object are also shown with the corresponding wrong labels (first upright, second rotated and correctly labelled by EfficientNet, and third rotated and incorrectly labelled by EfficientNet).

- Acoustic guitar: [link](#)

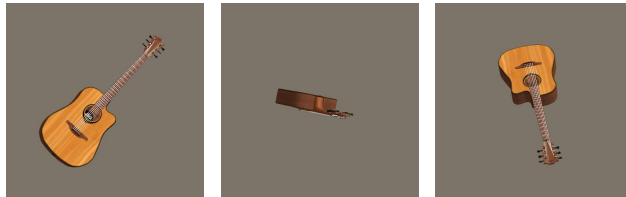


Figure 7. 1. Banjo, 2. Plectrum, 3. Whistle

- Airliner: [link](#)

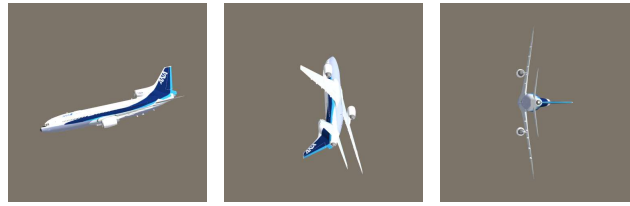


Figure 8. 1. Warplane, 2. Space shuttle, 3. Missile

- Backpack: [link](#)

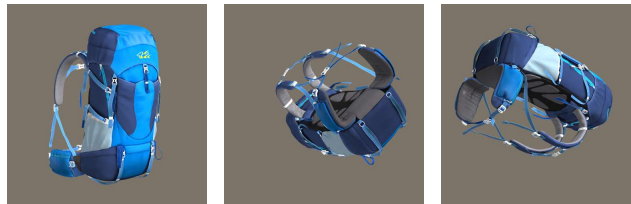


Figure 9. 1. Sleeping bag, 2. Neck brace, 3. Neck brace

- Binoculars: [link](#)



Figure 10. 1. Reflex camera, 2. Tripod

- Bow tie: object deleted

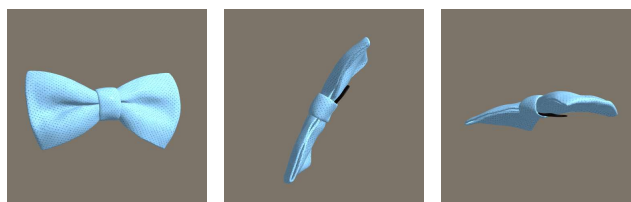


Figure 11. 1. Windsor tie, 2. Band Aid, 3. Hammerhead shark

- Cannon: [link](#)



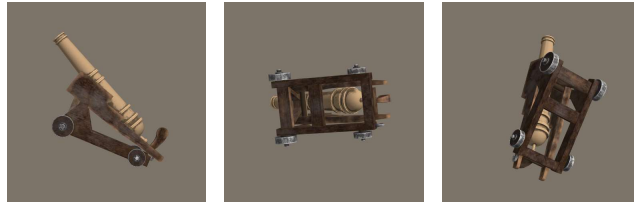


Figure 12. 1. Rifle, 2. Hourglass, 3. Guillotine

- Canoe: [link](#)



Figure 13. 1. Speedboat, 2. Hair slide, 3. Toaster

- Combination lock: [link](#)

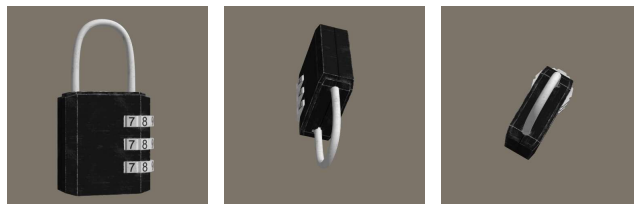


Figure 14. 1. Safe, 2. Hook, 3. Airship

- Corkscrew: [link](#)

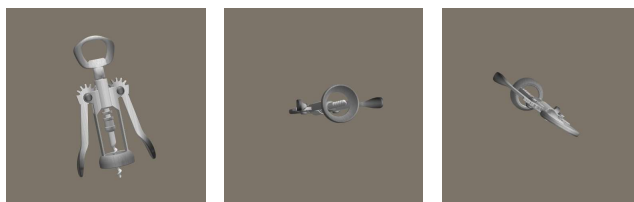


Figure 15. 1. Can opener, 2. Syringe, 3. Unicycle

- Crib: [link](#)



Figure 16. 1. Studio couch, 2. Plate rack, 3. Crate

- Dial telephone: [link](#)



Figure 17. 1. Smoothing iron, 2. Hook, 3. Joystick

- Digital watch: [link](#)



Figure 18. 1. Magnetic compass, 2. Buckle, 3. Chain

- Dumbbell: [link](#)



Figure 19. 1. Honeycomb, 2. Nail, 3. Honeycomb

- Electric fan: [link](#)



Figure 20. 1. Spotlight, 2. Microphone, 3. Strainer

- Frying Pan: [link](#)



Figure 21. 1. Spatula, 2. Gong, 3. Shield

- Fire engine: object deleted

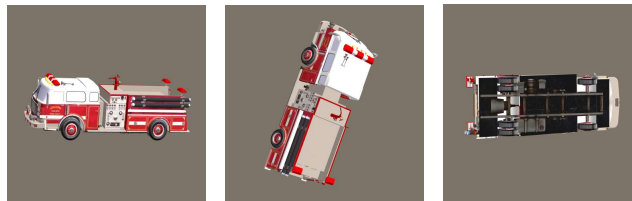


Figure 22. 1. Tow truck, 2. Trailer truck, 3. Chain

- Folding chair: [link](#)



Figure 23. 1. Rocking chair, 2. Tray, 3. Shovel

- Football helmet: [link](#)

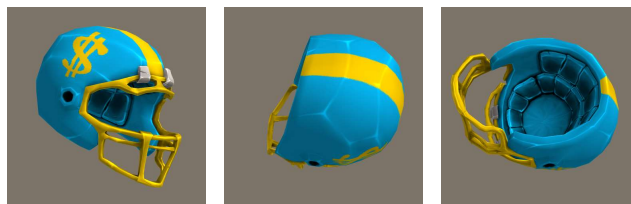


Figure 24. 1. Mask, 2. Balloon, 3. Bucket

- Forklift: [link](#)



Figure 25. 1. Crate, 2. Crane, 3. Lawn mower

- Garbage truck: object disabled

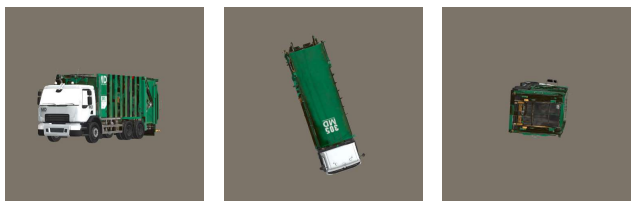


Figure 26. 1. Trailer truck, 2. Stretcher, 3. Racer

- Gasmask: [link](#)



Figure 27. 1. Ski mask, 2. Binoculars, 3. Spotlight

- Hair dryer: [link](#)



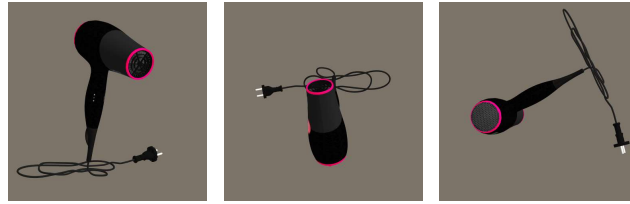


Figure 28. 1. Microphone, 2. Computer mouse, 3. Microphone

- Hammer: object deleted

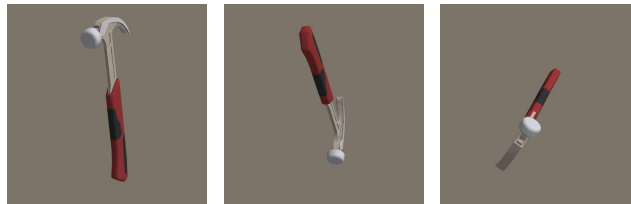


Figure 29. 1. Hatchet, 2. Can opener, 3. Bow

- Hatchet: [link](#)



Figure 30. 1. Hammer, 2. Cleaver, 3. Carpenter's plane

- Jellyfish: [link](#)

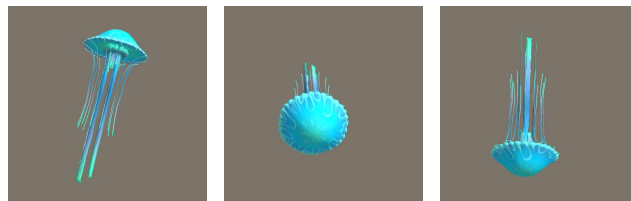


Figure 31. 1. Parachute, 2. Lampshade, 3. Lampshade

- Ladle: [link](#)

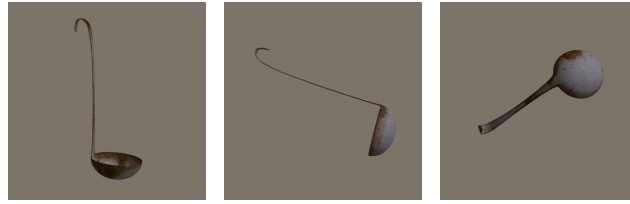


Figure 32. 1. Wooden spoon, 2. Maraca, 3. Safety pin

- Lawn mower: [link](#)

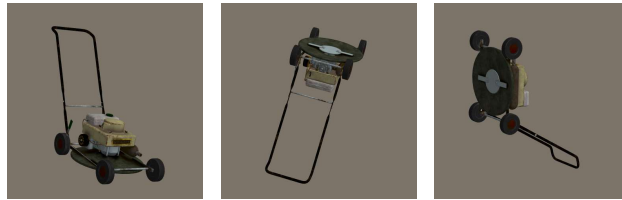


Figure 33. 1. Harvester, 2. Mousetrap, 3. Projector

- Mountain bike: [link](#)



Figure 34. 1. Tricycle, 2. Tricycle, 3. Unicycle

- Mountain tent: [link](#)

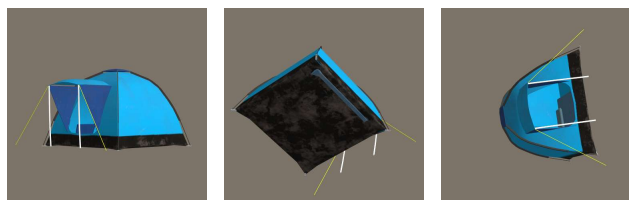


Figure 35. 1. Dome, 2. Sleeping bag, 3. Crash helmet

- Parachute: [link](#)

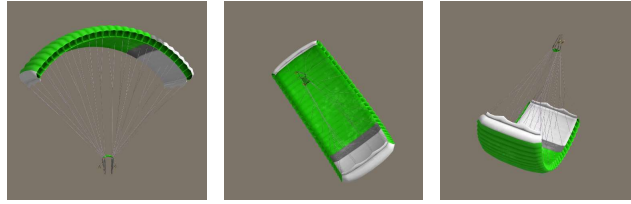


Figure 36. 1. Balloon, 2. Lighter, 3. Swing

- Park bench: [link](#)

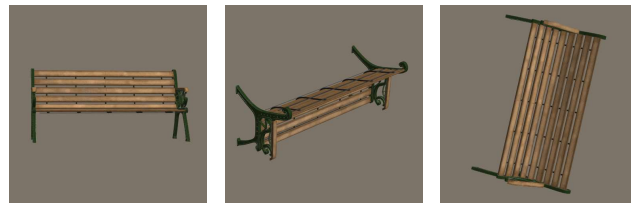


Figure 37. 1. Studio couch, 2. Paper towel, 3. Swing

- Piggy bank: [link](#)

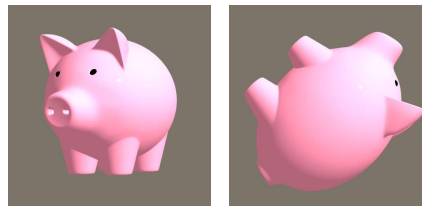


Figure 38. 1. Hog, 2. Teapot

- Pitcher: [link](#)

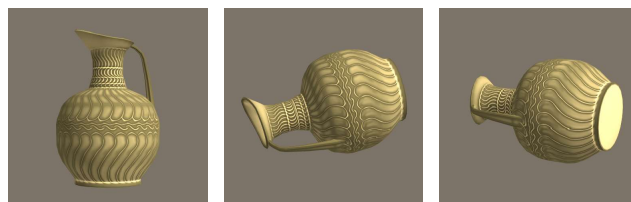


Figure 39. 1. Vase, 2. Conch, 3. Drum

- Power drill: [link](#)



Figure 40. 1. Hair dryer, 2. Screwdriver, 3. Mop

- Racket: [link](#)



Figure 41. 1. Strainer, 2. Ballpoint pen, 3. Mop

- Rocking chair: [link](#)



Figure 42. 1. Folding chair, 2. Throne, 3. Cradle

- Running shoe: object deleted



Figure 43. 1. Clog, 2. Honeycomb

- Scooter: [link](#)



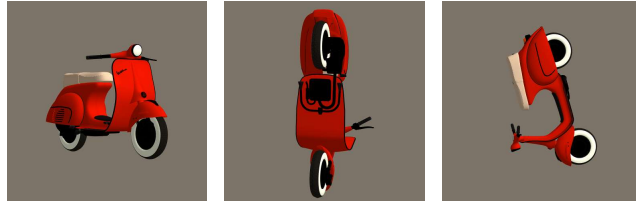


Figure 44. 1. Moped, 2. Moped, 3. Tricycle

- Shopping cart: [link](#)



Figure 45. 1. Shopping basket, 2. Shopping basket, 3. Shopping basket

- Stretcher: [link](#)

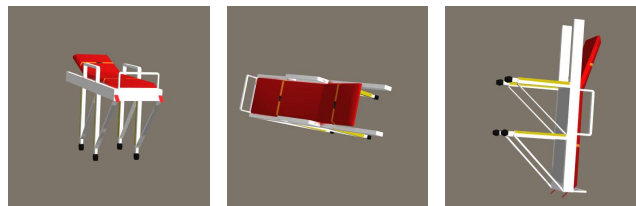


Figure 46. 1. Crutch, 2. Bobsled, 3. Matchstick

- Table lamp: [link](#)



Figure 47. 1. Pedestal, 2. Plunger, 3. Toilet seat

- Tank: [link](#)

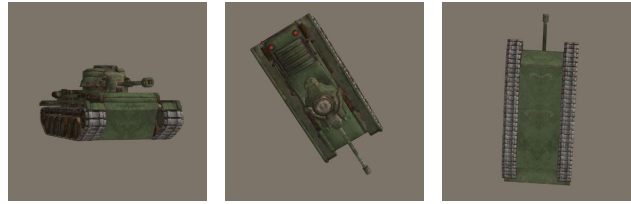


Figure 48. 1. Cannon, 2. Stretcher, 3. Pedestal

- Teapot: [link](#)



Figure 49. 1. Water jug, 2. Plunger, 3. Speaker

- Teddy bear: [link](#)

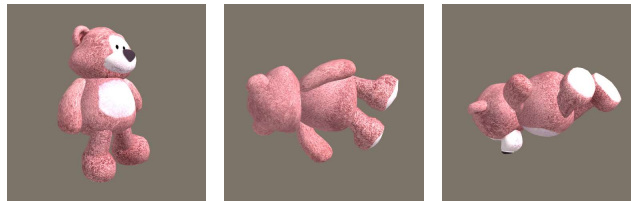


Figure 50. 1. Piggy bank, 2. Knot, 3. Piggy bank

- Tractor: [link](#)



Figure 51. 1. Forklift, 2. Mousetrap, 3. Forklift

- Traffic light: [link](#)



Figure 52. 1. Pole, 2. Missile, 3. Nail

- Trashcan: [link](#)



Figure 53. 1. Bucket, 2. Lighter, 3. Revolver

- Umbrella: [link](#)

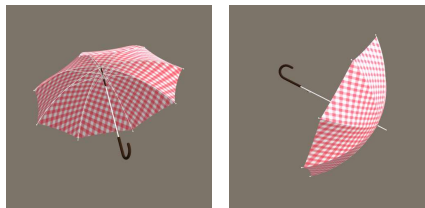


Figure 54. 1. Mountain tent, 2. Kimono

- Vacuum cleaner: [link](#)



Figure 55. 1. Lawn mower, 2. Chainsaw

- Violin: [link](#)

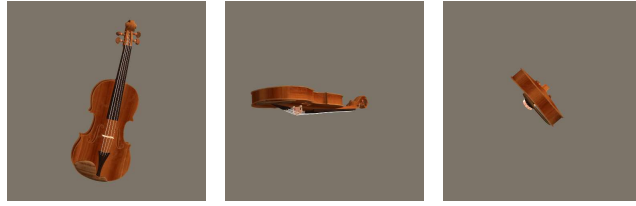


Figure 56. 1. Banjo, 2. Harp, 3. Spindle

- Wheelbarrow: [link](#)

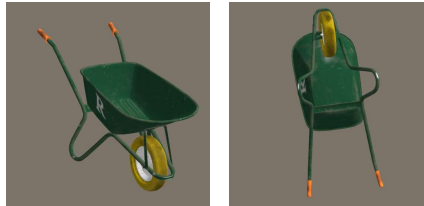


Figure 57. 1. Shovel, 2. Shovel